crystals

MDPI

Article

Effects of Changing Substituents on the Non-Linear Optical Properties of Two Coumarin Derivatives

Basílio Baseia [1,2,*], Francisco A. P. Osório [1,3], Larissa Ferreira Lima [2] and Clodoaldo Valverde [4,5,*]

1 Instituto de Física, Universidade Federal de Goiás, 74690-900 Goiânia, GO, Brazil; fosorio76@gmail.com
2 Departamento de Física, Universidade Federal da Paraíba, 58051-970 João Pessoa, PB, Brazil; larissa_ferreiralima@hotmail.com
3 Escola de Ciências Exatas e da Computação, Pontifícia Universidade Católica de Goiás, 74605-10 Goiânia, GO, Brazil
4 Campus de Ciências Exatas e Tecnológicas, Universidade Estadual de Goiás, 75001-970 Anápolis, GO, Brazil
5 Universidade Paulista, 74845-090 Goiânia, GO, Brazil
* Correspondence: basiliobaseia@yahoo.com.br (B.B.); valverde@ueg.br (C.V.)

Academic Editors: Ning Ye and Rukang Li
Received: 21 March 2017; Accepted: 25 May 2017; Published: 27 May 2017

Abstract: In this article, we study the electric properties of two coumarin derivatives whose difference stems from the change of substituents at 3-position of the pendant benzene ring ($C_{18}H_{15}NO_3$) and ($C_{18}H_{15}NO_4$). We use the supermolecule approach to deal with the molecules under the effect of the crystalline environment to calculate dipole moment, linear polarizability, and second-order hyperpolarizability, for the isolated and embedded molecules, including the static and dynamic cases and the presence of solvents. The (hyper) polarizabilities were derived from an iterative process and an ab initio computational procedure. In addition, we also calculated the HOMO-LUMO energies; at this point, the objective is to verify the effect of the exchange of substituents on the Band-Gap energy, an important parameter related to the excitation properties of coumarin compounds.

Keywords: non-linear optical properties; (hyper) polarizabilities; organic crystal; HOMO-LUMO energies

1. Introduction

Coumarin and its derivatives have been investigated by several authors in the last few years due to their application in the pharmaceutical industry as a precursor reagent in the synthesis of a number of synthetic anticoagulants [1]. Furthermore, coumarins display anticancer, antiviral, anti-inflammatory and anti-oxidant biological properties. Besides that, coumarin and its derivatives also work as well-known laser dyes [2–4] and useful probes in different photochemical and chemical studies. Most coumarins are highly fluorescent, a property that qualifies them for several applications, e.g., as high-efficiency dye-sensitized solar cells [5–7]. Other properties of coumarins come from an important building block, due to their synthetic accessibility and substitution variability. Also, in view of their structural diversity and potential applications in different areas of science, they play an important role in the modifications of different properties displayed by the introduction of different substituents into the heterocyclic ring.

Nonlinear optical (NLO) materials have attracted great attention due to their potential applications: among them we can cite signal processing for integrated optical applications and other sections of materials science and ultrafast optical communications [8–11]. This ultrafast response time feature enables the application of organic crystals in photonic devices [12–16]. Organic materials have been exhaustively studied since their non-linear optical properties can be better than those of inorganic ones.

In this work, we investigate the NLO properties of two coumarin derivatives, 6-methyl-N-(3-methilphenyl)-2-oxo-2H-chromene-3-carboxamide (compound I) and N-(3-methoxophenyl)-6-methyl-2-oxo-2H-chromene-3-carboxamide(compound II). The difference between these two compounds stems from the type of substituent at 3-position of the pendant benzene ring (see Figure 1). Our goal is the study of the effect caused by the change of coumarin substituents on the electric properties of the compounds I ($C_{18}H_{15}NO_3$) and compound II ($C_{18}H_{15}NO_4$). To this end, we calculate the dipole moment, the linear polarizability and the second hyperpolarizability for the isolated and embedded molecules of these two coumarins in the static and dynamic conditions. The molecular hyperpolarizabilities govern the behavior of the NLO process, such as the second harmonic generation, electro-optical effects and third harmonic generation. These processes have many applications, e.g., optical processing of information and optical computing, having great interest for state-of-the-art technology.

We will also consider the solvent media effect on the NLO dynamic properties of these compounds (Second Harmonic Generation (SHG), Kerr effect, dc-SHG) and, for this purpose, we calculate the HOMO and LUMO energies that are very important for determination of the excitation properties of the compounds.

2. Methodology

The two coumarin derivatives studied here, 6-methyl-N-(3-methylphenyl)-2-oxo-2H-chromene-3-carboxamide (compound I), structural formula $C_{18}H_{15}NO_3$ and *N*-(3-methoxyphenyl)-6-methyl-2-oxo-2*H*-chromene-3-carboxamide (compound II) $C_{18}H_{15}NO_4$, were synthesized and structurally characterized by Gomes et al. [17]. Compound I is crystallized in a monoclinic centrosymmetric space group $P2_1/c$. The main crystallographic data are: a = 7.2117(3) Å, b = 8.0491(3) Å, c = 23.6242(9) Å, $\alpha = 90^\circ$, $\beta = 94.388(4)^\circ$, $\gamma = 90^\circ$, unit cell volume $V = 1367.31(9)$Å^3 with four molecules in the unit cell. The compound II is crystallized in atriclinic centrosymmetric space group $P\bar{1}$ with the following crystallographic data: a = 7.1028(4) Å, b = 10.1367(4) Å, c = 10.8171(5) Å, $\alpha = 75.827(4)^\circ$, $\beta = 88.318(4)^\circ$, $\gamma = 71.271(4)^\circ$, unit cell volume $V = 714.10(6)$Å^3 with two molecules in the unit cell. The molecules exhibit an approximate planarity.

In this work, theoretical methods used to calculate the electric parameters were the Møller–Plesset Perturbation Theory (MP2) (dipole moment and linear polarizability) and the Density Functional Theory (DFT) at level $CAM-B3LYP$ (for the first hyperpolarizability (solvent medium) and second hyperpolarizability (crystal and solvent medium)). The $6-311+G(d)$ basis set was used for all atoms. All computational ab initio calculations were performed via Gaussian 09 software package [18].

The supermolecule (SM) approach was used to determine the effects of the crystalline environment polarization on the electrical properties of compounds I and II. The applicability of the SM approach is supported by its results close to the experimental ones [19–21]. Several recently published works use this technique due to the rapid convergence of NLO properties [22–27]. In the SM method, the atoms that form the surrounding molecules of the compounds are treated as point charges, since the interactions between molecules have a dominant electrostatic nature, taking into account long-range electrostatic effects [28,29]. Another alternative model to estimate $\chi^{(1)}$ and $\chi^{(2)}$ was proposed by Seidler and Champagne [30–35] with very good results.

Using an iterative process in which the electrical polarization effects are considered, we have as a major goal the determination of the linear and nonlinear electrical properties of compounds I and II, both for isolated and embedded molecules. To this end, we started (step zero) with the calculation of partial atomic charges for one isolated molecule of the asymmetric unit using the CHELPG scheme (Charges from Electrostatic Potentials using a Grid-based method); this scheme is based on the calculation of atomic charges, which are fitted to reproduce the molecular electrostatic potential at a number of points in the vicinity of the molecule [18], obtained from the 6-311 + G(d) basis set at the MP2 level and described by its charge distribution in a vacuum. Then, (i) we calculated the partial atomic charges (CHELPG) for a single isolated molecule; (ii) in the position of each corresponding

atom in the generated unit cells, we replaced the atom by its partial atomic charge obtained in item (i); (iii) we calculated the static electric properties (dipole moment and second hyperpolarizability), as well as the new partial atomic charges of the asymmetric unit; (iv) we returned to item (ii) and repeated the procedure until convergence in the electric properties of the molecule is achieved, as implemented in previous works using this procedure [20,21,27]. To simulate the embedded molecules of compound I, we consider a unit cell with four asymmetric units (37 atoms in each unit) in a spatial configuration of $9 \times 9 \times 9$, totalizing 729 unit cells with 107,892 atoms. For compound II, a similar configuration was employed but with two asymmetric units in each unit cell (38 atom in each unit), totalizing 55,404 atoms.

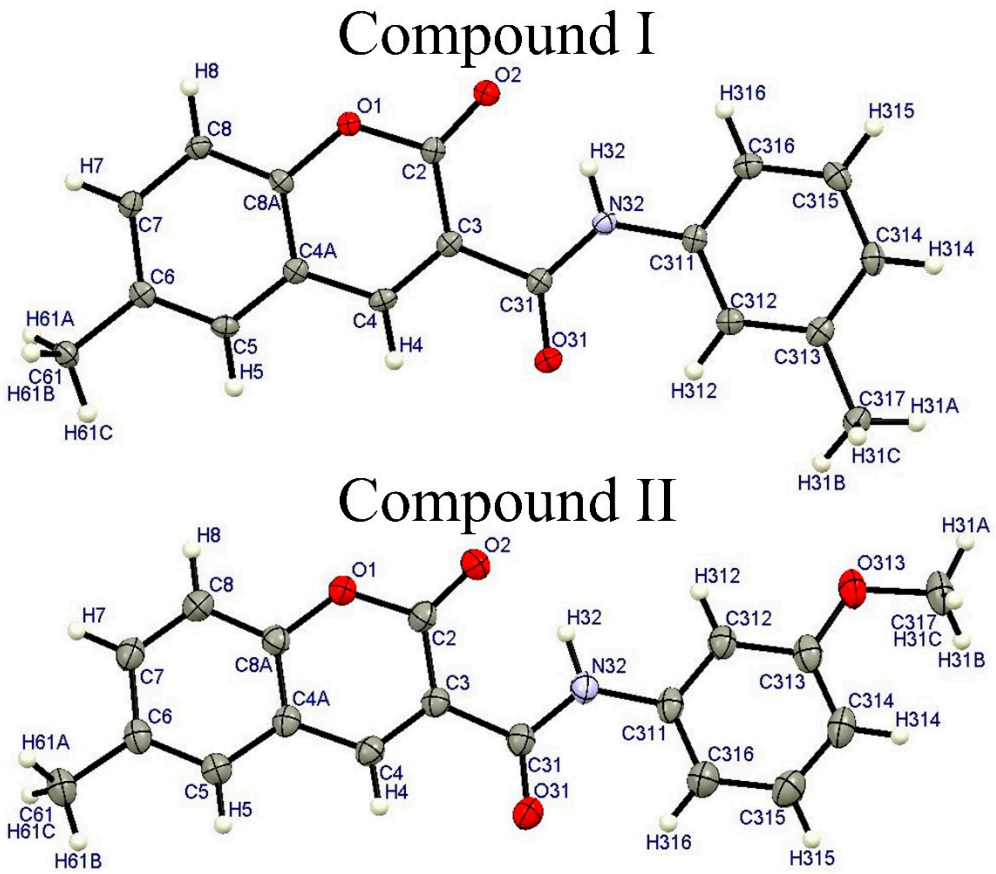

Figure 1. A view of the asymmetric unit of the compounds I and II with the atom-numbering scheme.

In the present study, the electric dipole moment, linear average polarizability ($\langle\alpha\rangle$), and anisotropy of polarizability ($\Delta\alpha$) of the compounds have been calculated via the following expression,

$$\mu = \left(\mu_x^2 + \mu_y^2 + \mu_z^2\right)^{\frac{1}{2}}, \tag{1}$$

$$\langle\alpha\rangle = \frac{\alpha_{xx} + \alpha_{yy} + \alpha_{zz}}{3}, \tag{2}$$

$$\Delta\alpha = 2^{\frac{-1}{2}}\left[\left(\alpha_{xx} - \alpha_{yy}\right)^2 + \left(\alpha_{yy} - \alpha_{zz}\right)^2 + \left(\alpha_{zz} - \alpha_{xx}\right)^2 + 6{\alpha_{xz}}^2 + 6{\alpha_{xy}}^2 + 6{\alpha_{yz}}^2\right]^{\frac{1}{2}}. \tag{3}$$

The total first hyperpolarizability is given by,

$$\beta_{total} = \sqrt{{\beta_x}^2 + {\beta_y}^2 + {\beta_z}^2}, \tag{4}$$

with $\beta_x = (\beta_{xxx} + \beta_{xyy} + \beta_{xzz})$; $\beta_y = (\beta_{yyy} + \beta_{yxx} + \beta_{yzz})$ and $\beta_z = (\beta_{zxx} + \beta_{zyy} + \beta_{zzz})$ and the average of the second hyperpolarizability is reached by,

$$\langle \gamma \rangle = \frac{1}{15} \sum_{i,j=x,y,z} (\gamma_{iijj} + \gamma_{ijij} + \gamma_{ijji}). \quad (5)$$

Since in the present work optical dispersion was not taken into account, the value (or absolute value) of static average second hyperpolarizability can be simplified via the use of Kleinmann [36] and calculated through the expression,

$$\langle \gamma \rangle = \frac{1}{5} [\gamma_{xxxx} + \gamma_{yyyy} + \gamma_{zzzz} + 2(\gamma_{xxyy} + \gamma_{xxzz} + \gamma_{yyzz})]. \quad (6)$$

All the numerical results of the tensors standing for polarizability and hyperpolarizabilities were obtained from the Gaussian 09 output file and converted to the electronic units (esu), where the molecular environment was taken into account through the supermolecule method (SM).

3. Results and Discussion

Table 1 shows the results of our theoretical calculations obtained via the MP2 with 6-311 $+G(d)$ basis set for the dipole moment components and average dipole moment for the two coumarin derivatives. The different substituents in the coumarin molecular structure at the 3-position of the pendant benzene ring, identified by letter C in Figure 2, are CH_3 (Me) and OCH_3 (OMe). The results in Table 1 stand for both the isolated and embedded molecules. The compounds with the substituent methyl (Me) and methoxy (OMe) are denoted as compound I and compound II, respectively. As can be seen for the isolated molecule, the substitution of the substituent Me by OMe causes a decrease in the value of average dipole moment from 4.25D to 3.19D, a reduction of 1.06D (∼25%). Decreases in the value of the average dipole moment were also observed for the compounds in the crystalline phase: in this case, the value of $\overline{\mu}$ went from 5.05D to 3.92D, a reduction of 1.13D (∼29%). For both compounds, the effect of the environment polarization increases the value of $\overline{\mu}$ of 0.8D (Me) and 0.73D (OMe) when compared with the results for the isolated molecule.

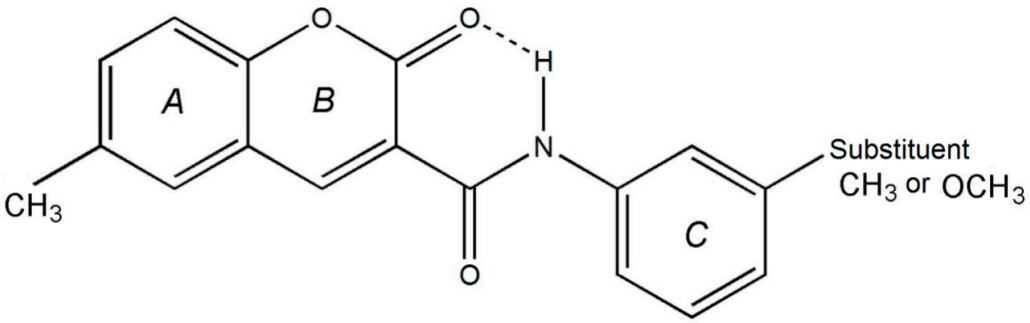

Figure 2. Substituent at the 3-position of the pendant benzene ring identified by letter C [17].

From Table 1, it can be noted that for the isolated molecule of compound I the component μ_x of dipole moment is only slightly greater than the other components. The effect of changing the substituent is to modify the equilibrium of the dipole moment components, i.e., the components μ_x and μ_z have their values reduced while the value of μ_y shows a growth. This effect is also observed in the crystalline phase of the compounds.

Table 2 present the results for the components (α_{ij}) of the linear polarizability and its average value ($\langle \alpha \rangle$) for the compounds I and II, for isolated and embedded molecules. As it can be noted, the change of substituents causes a small variation in the values of linear polarizability components as well as in the values of average linear polarizability. However, the anisotropy of the linear polarizability

decreases significantly when the substituent Me is replaced by OMe, showing a variation of 49% as displayed in Table 2 for both isolated and embedded molecules, respectively. As can be observed for both substituents, the diagonal components of the linear polarizability dominate the polarizability. For compound II, particularly, component α_{yy} dominates, which indicates a substantial delocalization of charges in that direction due to the change of substituents.

Table 1. MP2/6-311 + G(d) results for the components of the dipole moment (D).

Isolated Molecule	μ_x	μ_y	μ_z	$\langle\mu\rangle$
Me	−2.65	−2.37	−2.32	4.25
OMe	−0.92	−2.86	−1.06	3.19
Embedded Molecule	μ_x	μ_y	μ_z	$\langle\mu\rangle$
Me	−3.06	−2.25	−3.33	5.05
OMe	−1.24	−3.52	−1.18	3.92

Table 2. MP2/6-311 + G(d) results for the linear polarizability (10^{-24} esu).

Isolated	α_{xx}	α_{xy}	α_{yy}	α_{xz}	α_{yz}	α_{zz}	$\langle\alpha\rangle$	$\Delta\alpha$
Me	36.00	8.32	28.86	6.61	15.19	36.88	33.91	62.94
OMe	18.97	6.33	49.42	5.31	10.86	35.72	34.70	42.20
Embedded	α_{xx}	α_{xy}	α_{yy}	α_{xz}	α_{yz}	α_{zz}	$\langle\alpha\rangle$	$\Delta\alpha$
Me	36.08	8.43	29.10	6.72	15.20	37.01	34.06	62.82
OMe	19.09	6.34	49.32	5.37	10.92	35.75	34.72	42.16

Table 3 display the results obtained through the use of DFT ($CAM-B3LYP$) with 6-311 + $G(d)$ basis set for the components $\left(\gamma_{ijkl}\right)$ of second hyperpolarizability and for the average second hyperpolarizability ($\langle\gamma\rangle$), both for the title compound with the substituent Me and OMe and for the isolated and embedded molecules respectively. As can be noted, the value of the average second hyperpolarizability presents a decrease of 5% for isolated molecules and of 17% for the embedded one, due to the change of substituent, Me replaced by OMe, in the coumarin derivatives. Also, when the results for isolated molecules are compared with those for embedded ones, the effects of the crystalline polarization are seen to be causing significant reductions in the $\langle\gamma\rangle$-values, of 9.4% for compound I and of 21.6% for compound II, respectively.

Only the values of the components γ_{yyyy} and γ_{yyzz} increase due to the change of substituent, from Me to OMe, which is accompanied by a reduction in the other components. The greatest variation was observed in the value of γ_{yyyy} of 141% for the isolated molecule and 105% for the embedded molecule. As previously noted for the dipole moment, linear polarizability and also for the second hyperpolarizability, the replacement of the substituent causes a greater distortion of the electron cloud in the y-direction for both isolated and embedded molecules.

Table 3. CAM-B3LYP/6-311 + G(d) results for the second hyperpolarizability (10^{-36} esu) in the static case.

Isolated	γ_{xxxx}	γ_{yyyy}	γ_{zzzz}	γ_{xxyy}	γ_{yyzz}	γ_{xxzz}	$\langle\gamma\rangle$
Me	22.80	49.65	117.37	21.70	63.10	33.80	85.41
OMe	12.42	119.71	67.36	14.69	75.81	12.76	81.20
Embedded	γ_{xxxx}	γ_{yyyy}	γ_{zzzz}	γ_{xxyy}	γ_{yyzz}	γ_{xxzz}	$\langle\gamma\rangle$
Me	21.76	46.14	108.52	19.42	57.43	30.07	78.05
OMe	12.68	94.51	58.53	12.37	60.55	11.24	66.80

In sum, in the static case (ω = 0.0) the values of electrical parameters for the isolated molecules are $\overline{\mu} = 4.25$D, $\overline{\alpha} = 33.91 \times 10^{-24}$ esu, and $\overline{\gamma} = 85.41 \times 10^{-36}$ esu for compound I, whereas $\overline{\mu} = 3.19$D, $\overline{\alpha} = 34.70 \times 10^{-24}$ esu, and $\overline{\gamma} = 81.2 \times 10^{-36}$ esu for compound II. Urea is one of prototypical molecules used for the purpose of comparison in the study of NLO properties of molecular systems. It has been used frequently as a threshold value of the NLO parameters. As can be noted, the values of all parameters for the compounds studied here are greater than those values found for the urea parameters ($\overline{\mu} = 1.37$D, $\overline{\alpha} = 3.83 \times 10^{-24}$ esu, and $\overline{\gamma} = 4.16 \times 10^{-36}$ esu) [37–39]. When our results are compared with those of urea, compound I is 3.1 times greater for the dipole moment, 8.8 times greater for the average linear polarizability and 20.5 times greater for the second hyperpolarizability, while compound II is 2.3 times larger for the dipole moment, 9.0 times greater for linear polarizability, and 19.5 times greater for the average value of the second hyperpolarizability.

Comparing our results with those obtained by other authors for coumarin derivatives, the values in the present study were: $\overline{\mu} = 3.86$D, $\overline{\alpha} = 23.37 \times 10^{-24}$ esu, and $\overline{\gamma} = 22.34 \times 10^{-36}$ esu) for the 3-Acetyl-6-Bromocoumarin [27]; our results for the dipole moment, average linear polarizability, and average second hyperpolarizability for compound I are 1.1, 1.45, and 3.8 times higher, respectively; for compound II the values are 3.1 times smaller for the dipole moment, 1.5 times greater for the average linear polarizability and 3.6 times greater for the average value of the second hyperpolarizability. For the 6-bromo-4chloro-3-formyl coumarin isolated molecule, the NLO parameters of Raj et al. [40] are $\overline{\mu} = 4.17$D, $\overline{\alpha} = 147.73 \times 10^{-24}$ esu, and $\overline{\beta} = 8.12 \times 10^{-30}$ esu, and the average linear polarizability of this compound is four times greater than that obtained for the coumarin derivatives studied here; however, the second hyperpolarizability was not calculated in Ref. [40].

Figures 3 and 4, for compounds I and II respectively, present our results for the dynamic average value of the linear polarizability $\langle \alpha(-\omega, \omega) \rangle$ and for the average values of the second hyperpolarizabilities, $\langle \gamma(-\omega; \omega, 0, 0) \rangle$ and $\langle \gamma(-2\omega; \omega, \omega, 0) \rangle$, for both isolated and embedded molecules. It can be observed that the dispersion relations for $\langle \alpha(-\omega, \omega) \rangle$ for both compounds present a smooth curve when the frequency increases, whereas the value of the average linear polarizability for isolated and embedded molecules presents no significant difference for both compounds. However, the influence of the crystalline environment on $\langle \gamma(-\omega; \omega, 0, 0) \rangle$, which comes from the Kerr effect, is more prominent: when the frequency increases, the value $\langle \gamma(-\omega; \omega, 0, 0) \rangle$ is reduced for the isolated molecule, and this effect is more significant for compound II.

More complex is the dispersion relationship of the average second hyperpolarizability $\langle \gamma(-2\omega; \omega, \omega, 0) \rangle$ denoting the dc-SHG. As observed in Figures 3 and 4, the dc-SHG spectra show sharp peaks in the region of high frequencies ($\omega > 0.07$ a.u.) for both compounds. In these figures, the insets display more details in the dispersion relation for $\omega < 0.06$ a.u., a region of great interest for experimentalists. As we can see, the $< \gamma >$-values for the isolated molecules are greater than those for the embedded ones: for $\omega = 0.06$ a.u. the difference is of 50%. We also compared the compound I embed ded molecule (crystal) at the frequency of ω = 0.085 a.u., with the compound I isolated molecule in the static case, where an increase of 467,378% was shown (see Figure 3), indicating that the resonance frequency belongs to the interval 0.08–0.09 a.u., while in compound II it belongs to the interval 0.072–0.08 a.u. (see Figure 4); this fact concerns the replacement of the methyl (Me) substituent by the methoxy (OMe) substituent.

An analysis of molecular systems in solvent medium is of great importance, due to the fact that solvent medium affects the properties of molecules, of which we can cite: ground state geometry, energy levels, dipole moment, linear polarizabilities, first and second hyperpolarizabilities. This work used an implicit solvation scheme based on the formalism of the integral PCM equation (PCM-IEF). To complete our studies, we considered the effects of various solvent media (gas-phase (ε = 1.00), chloroform (ε = 4.71), dichloromethane (ε = 8.93), acetone (ε = 20.49), ethanol (ε = 24.85), methanol (ε = 32.61), dimethyl sulfoxide (ε = 46.70), and water (ε = 78.36)) on the dynamic electrical properties of compounds I and II, where ε is the medium dielectric constant. In these cases, the compounds lose their center-symmetry conformation while presenting the first hyperpolarizability value not null. In Table 4,

the results for the dynamic linear polarizability $\alpha(-\omega;\omega)$ for $\omega = 0.04282$ a.u., for the compounds I and II in gas-phase and various solvent media are shown. It is notable that the values of $\alpha(-\omega;\omega)$ are greater for compound II with the substituent OMe; however, the differences due to the change of substituents are small, around ~2%.

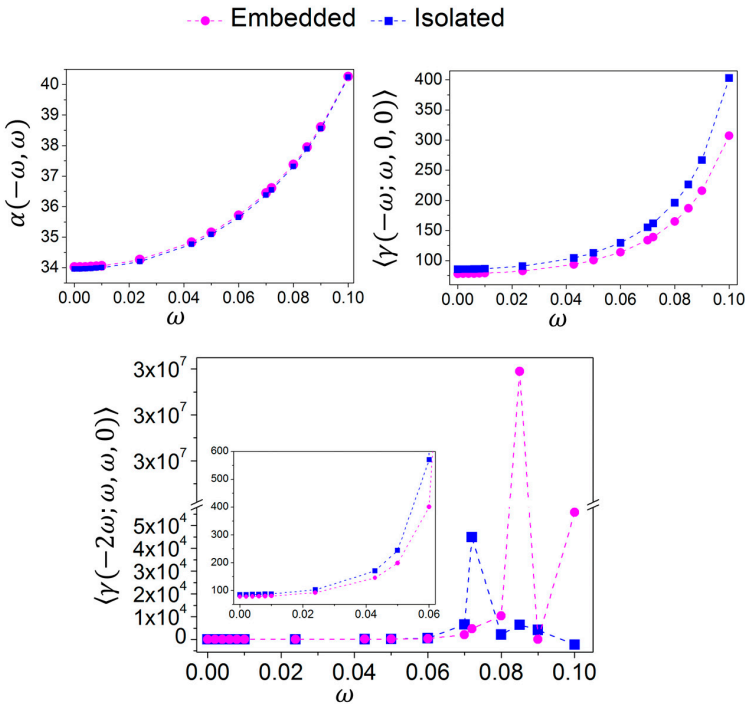

Figure 3. Dynamic evolution of the calculated values for the average linear polarizability (10^{-24} esu) and average second hyperpolarizability (10^{-26} esu) for compound I.

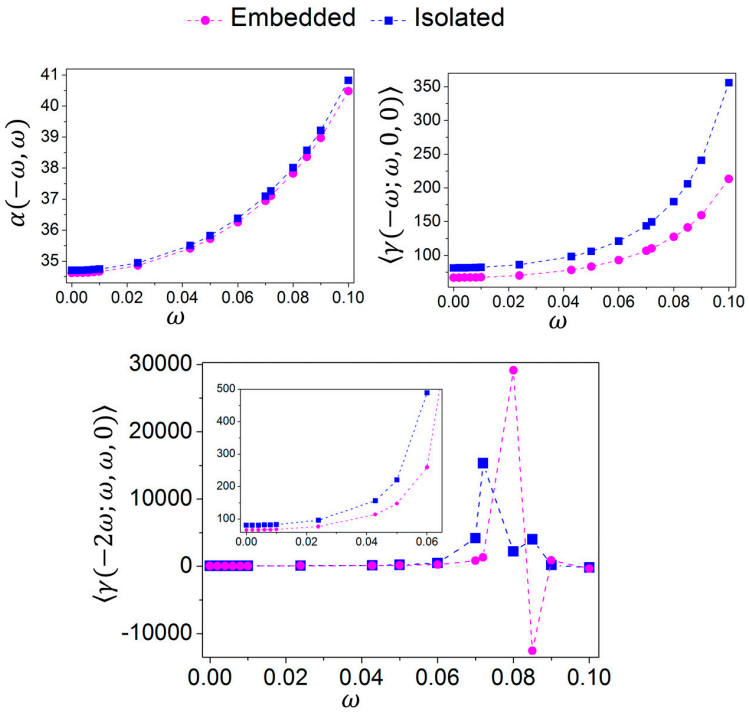

Figure 4. Dynamic evolution of the calculated values for the average linear polarizability (10^{-24} esu) and average second hyperpolarizability (10^{-26} esu) for compound II.

Table 4. CAM-B3LYP/6-311 + G(d) results for the dynamic linear polarizability (10^{-24} esu) for compounds I and II, with the substituents Me and OMe respectively.

$\alpha(-\omega;\omega)$	Me	OMe
Acetone	40.92	41.80
Chloroform	41.61	42.49
Dichloromethane	41.45	42.33
DiMethylSulfoxide	41.41	42.29
Ethanol	40.94	41.83
Gas-Phase	36.93	37.85
Methanol	40.65	41.54
Water	40.70	41.59

The replacement of the methyl substituent by methoxy increases the average linear polarizability in all solvent media; see Figure 5.

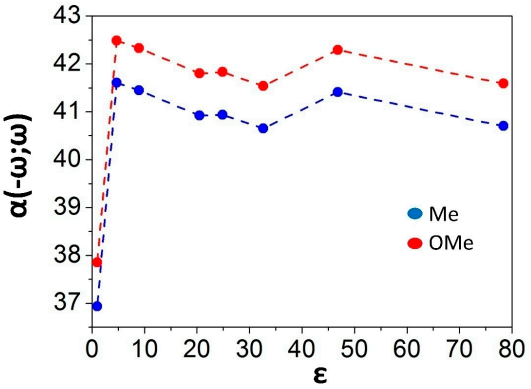

Figure 5. PCM-CAM-B3LYP/6-311 + G(d) results for average linear polarizability (10^{-24} esu) for $\omega = 0.04282$ a.u. of compounds I and II in gas-phase (ε = 1.00), chloroform (ε = 4.71), dichloromethane (ε = 8.93), acetone (ε = 20.49), ethanol (ε = 24.85), methanol (ε = 32.61), dimethyl sulfoxide (ε = 46.70), and water (ε = 78.36); ε stands for the dielectric constant.

In Table 5, we present the results for the dynamic first hyperpolarizabilities $\beta_{\|}z(-2\omega;\omega,\omega)$ and $\beta_{\|}z(-\omega;\omega,0)$ for $\omega = 0.04282$ a.u. These parameters are the projection of the first hyperpolarizability in the dipole moment direction. We first analyze the effects of the constituent change on the function $\beta_{\|}z(-2\omega;\omega,\omega)$ that denotes the SHG. It can be seen that all the values of this function for compound I are negatives for all the solvent media, i.e., its components are anti-parallel to the dipole moment vector; for compound II, the values of $\beta_{\|}z(-2\omega;\omega,\omega)$ are negative only for the Gas-phase and Chloroform. However, the absolute variation of $\beta-$ SHG due to the change of substituent is practically constant ($\sim 4 \times 10^{-30}$ esu). It is expected that the higher the first hyperpolarizability value, the greater will be the probability of the molecular system being a NLO material. The swap of the Me substituent to OMe increases the first hyperpolarizability values in all solvent media, see Figure 6.

As can be seen in Table 6, all the values of $\langle\gamma(-2\omega;\omega,\omega,0)\rangle$ for $\omega = 0.04282$ a.u. present a reduction due to the change of substituent from Me to OMe in the coumarin derivatives. Comparison of this effect for the several solvent media is shown in Table 6; it can be observed that the smallest reduction in the Gama-value occurs for Gas-phase. Also, from Table 6 the values of $\langle\gamma(-\omega;\omega,0,0)\rangle$ are shown to present a small variation with the change of substituent, while the γ-*values* increase 2.8% except for the Gas-phase where the variation is smaller, around 1%.

Table 5. CAM-B3LYP/6-311 + G(d) results for the dynamic first hyperpolarizability (10^{-30} esu) for the compounds I and II, with the substituent Me and OMe respectively.

	$\mathbf{fi}_{\|}z(-2!;!,!)$		$\mathbf{fi}_{\|}z(-!;!,0)$	
	Me	**OMe**	**Me**	**OMe**
Acetone	−3.85	0.90	−1.55	2.43
Chloroform	−6.19	−0.83	−2.99	1.08
Dichloromethane	−4.83	0.26	−2.15	1.91
DiMethylSulfoxide	−3.52	1.35	−1.28	2.79
Ethanol	−3.73	1.01	−1.46	2.52
Gas-Phase	−1.02	−5.68	−5.51	−2.43
Methanol	−3.56	1.08	−1.36	2.57
Water	−3.30	1.29	−1.18	2.76

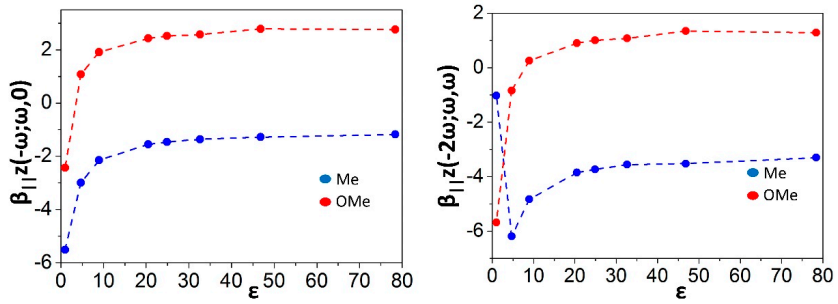

Figure 6. PCM-CAM-B3LYP/6-311 + G(d): results for first hyperpolarizabilities (10^{-30} esu) $\boldsymbol{\beta}_{\|}z(-\boldsymbol{\omega};\boldsymbol{\omega},\mathbf{0})$ and $\boldsymbol{\beta}_{\|}z(-\mathbf{2}\boldsymbol{\omega};\boldsymbol{\omega},\boldsymbol{\omega})$ for $\omega = 0.04282$ a.u. of compounds I and II in gas-phase (ε = 1.00), chloroform (ε = 4.71), dichloromethane (ε = 8.93), acetone (ε = 20.49), ethanol (ε = 24.85), methanol (ε = 32.61), dimethyl sulfoxide (ε = 46.70), and water (ε = 78.36).

Table 6. CAM-B3LYP/6-311 + G(d) results for the dynamic second hyperpolarizability (10^{-36} esu) for compounds I and II, with the substituent Me and OMe respectively, for $\omega = 0.04282$ a.u.

	$\boldsymbol{\gamma(-2\omega;\omega,\omega,0)}$		$\boldsymbol{\gamma(-\omega;\omega,0,0)}$	
	Me	**OMe**	**Me**	**OMe**
Acetone	233.44	224.69	166.82	162.19
Chloroform	247.44	237.56	163.20	158.71
Dichloromethane	242.84	233.33	166.97	162.27
DiMethylSulfoxide	240.10	230.98	171.65	166.80
Ethanol	233.56	224.82	167.44	162.78
Gas-Phase	187.58	182.97	112.48	111.30
Methanol	229.15	220.73	166.09	161.51
Water	229.41	221.01	167.41	162.79

The substitution of the methyl substituent with methoxy increased the linear polarizability and the first hyperpolarizability, but decreased the second hyperpolarizability in all solvents; this is due to the fact that the substituents are attached to the aromatic ring: in this case the methyl has an electron donor effect, whereas the methoxy (OMe), which is more electronegative, acts as an inducer; see Figure 7.

The overlap of the embedded structure and gas-phase molecule of compounds I and II occurs by pendant benzene ring anchorage point, shown in Figure 8. The X-ray geometries and the theoretical structure were analyzed in terms of the root mean square deviation (RMSD) calculated for non-H atoms. The H atoms were disregarded in view of their uncertainties in X-ray position refinement. The compounds I and II present a RMSD = 0.0846 and max. d = 0.1532 Å and RMSD: 0.0779; max. d = 0.1808 Å, respectively. Both RMSD parameters indicate no deviation between theoretical and experimental data.

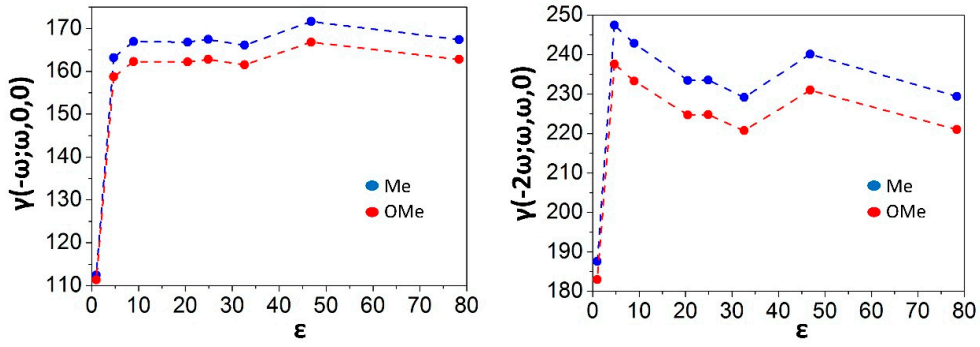

Figure 7. PCM-CAM-B3LYP/6-311 + G(d) results for second hyperpolarizabilities (10^{-36} esu) $\langle\gamma(-\omega;\omega,0,0)\rangle$ and $\langle\gamma(-2\omega;\omega,\omega,0)\rangle$ for $\omega = 0.04282$ a.u. of compounds I and II in gas-phase (ε = 1.00), chloroform (ε = 4.71), dichloromethane (ε = 8.93), acetone (ε = 20.49), ethanol (ε = 24.85), methanol (ε = 32.61), dimethyl sulfoxide (ε = 46.70), and water (ε = 78.36).

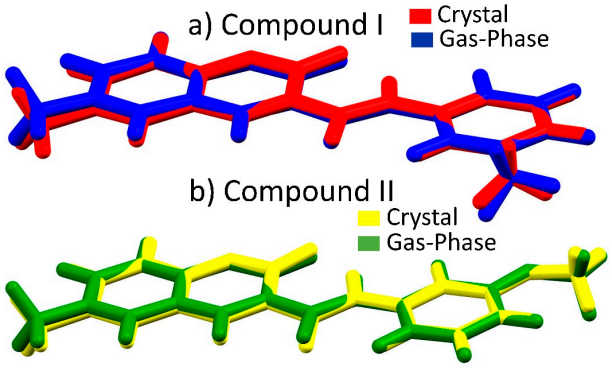

Figure 8. (**a**) Compound I overlap of compound I red (crystal), blue (gas-phase) and (**b**) compound II yellow (crystal) and green (gas-phase). The anchorage point was the pendant benzene ring region.

4. Frontier Molecular Orbitals

The calculation of the frontier molecular orbital energies (HOMO and LUMO) is very important because these energies are related to the excitation properties of the coumarin compounds studied here. The differences between HOMO-LUMO energies are called "Band-Gap energy": when the Band-Gap energy of the compound is greater than 3.1 eV the maximum absorption wavelengths (λ_{max}) fall into the ultra violet (UV) region. As we can note from Figure 9 and Tables ES1–ES3 (Electronic Supplementary Information), the differences due to the change of substituent in the coumarin derivatives cause no remarkable change in the "gap energies" for all solvent media. Only for the gas-phase is the Band-Gap energy smaller than 6.0eV for the solvent media, and the Band-Gap energies are greater than 6 eV; however, the change of substituent in the coumarin derivatives causes variations of less than 0.68%.

Due to the fact that methyl (Me) has an electron-donor effect and methoxyl (OMe) is more electronegative, the Band-Gap energy in all solvent media is small in the compound containing methoxyl (compound II); this explains why the first hyperpolarizability is greater in this compound II, see Figure 6, since a small Band-Gap energy value is indicative of a good NLO property of the compound.

The ionization energy (E_I), electron affinity (E_A), the electronic chemical potential (μ_{cp}) and the chemical hardness (η) can be expressed through HOMO and LUMO orbital energies as $E_I = -E_{HOMO}$; $E_A = -E_{LUMO}$; $\mu_{cp} = \frac{1}{2}(E_{HOMO} + E_{LUMO})$ and $\eta = \frac{1}{2}(E_{LUMO} - E_{HOMO})$. These global quantities can be used as complementary tools in the description of thermodynamic aspects of chemical reactivity in connection with minimum polarizability and maximum hardness principles. For our two coumarin

derivative compounds, we can note that the values of these chemical descriptors present small variation with the change of substituent, both in the gas-phase and in the presence of solvents.

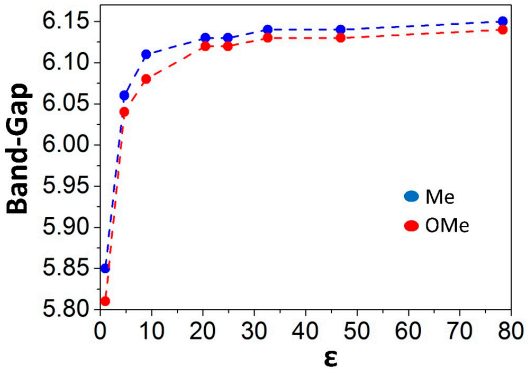

Figure 9. PCM-CAM-B3LYP/6-311 + G(d) results for the energy Band-Gap (in eV) of compound I and II in gas-phase (ε = 1.00), chloroform (ε = 4.71), dichloromethane (ε = 8.93), acetone (ε= 20.49), ethanol (ε = 24.85), methanol (ε = 32.61), dimethyl sulfoxide (ε = 46.70), and water (ε = 78.36).

One of the parameters used to control the NLO properties of organic compounds is the Band-Gap energy; this is done, for example, by modifying the structure with the replacement of a substituent; another way would be by the inclusion of solvents. These modifications allow us to increase or decrease the Band-Gap; see Figure 10. Checking the Band-Gap values in gas-phase and in dimethyl sulfoxide (DMSO) media, Figure 10, we have an increase of 4.96% for Me and of 5.51% for OMe. The effect of the transition between a non-polar solvent (chloroform) and a polar solvent (DMSO) does not significantly affect the Band-Gap energy values, as can be seen from Figure 10, where the differences between the chloroform-DMSO did not exceed 0.08 eV for Me and 0.09 eV for OMe. The HOMO-LUMO energy Band-Gap is just one of several parameters that influence the molecule.

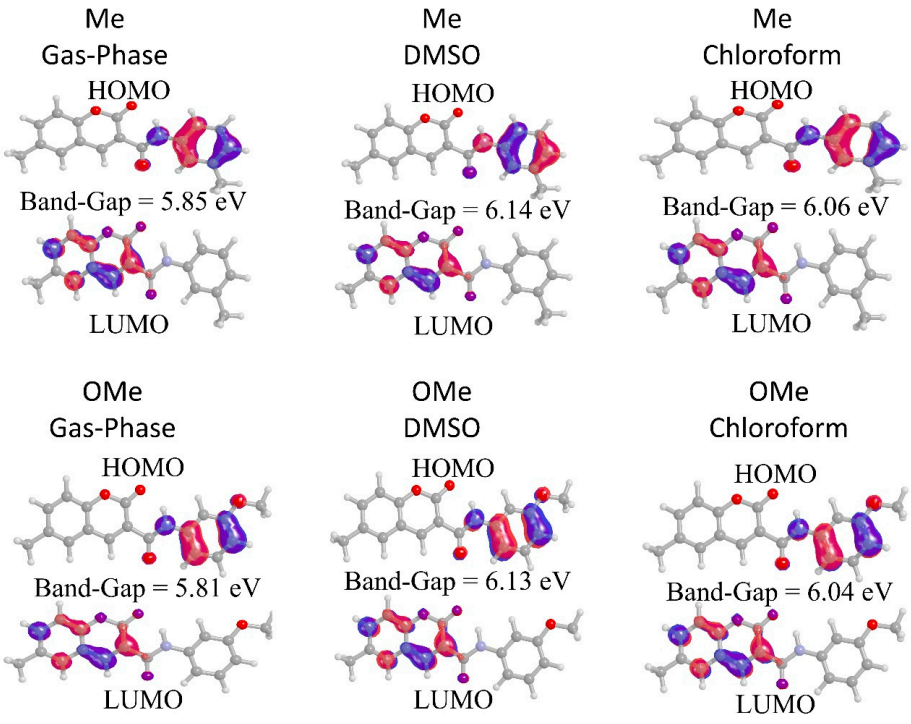

Figure 10. The HOMO-LUMO frontier orbitals for the coumarin compounds I and II in three different solvent media.

5. Conclusions

In the present work, we investigated the linear and non-linear optical (NLO) properties of two coumarin derivatives: *6-methyl-N-(3-methilphenyl)-2-oxo-2H-chromene-3-carboxamide* (compound I) and *N-(3-methoxophenyl)-6-methyl-2-oxo-2H-chromene-3-carboxamide* (compound II). The difference between these two compounds stems from the type of substituent at 3-position of the pendant benzene ring (see Figure 1) and this is exactly the behavior exploited here, the effect of the change of substituent on the electric properties of these compounds. Therefore, the average linear polarizability and the first and second hyperpolarizabilities were calculated via the MP2 and (DFT) CAM-B3LYP with the 6-311 $+G(d)$ basis set both in static and dynamic cases. Our calculations were made for the isolated molecules in the absence and in the presence of the solvent media. Also, the various effects of the crystalline environment polarization on the electric parameters of the compounds were considered. As the substituents are bonded to the aromatic ring, the methyl (Me) has an electron donor effect and the methoxyl (OMe), which is more electronegative, acts as inducer and resonant donor due to unpaired electron pairs; this causes a decrease in the density of the benzene ring, leading to a higher polarity for the benzene ring containing a methoxyl molecule.

In the static case, almost all values of electric parameters of compound I (substituent Me) are greater than those of compound II (substituent OMe), the exception occurring for the value of average linear polarizability of compound II, which is a little bigger. As an example, the substitution of Me with OMe causes in the crystal a reduction of 29% in the dipole moment; a reduction of 17% in the average second hyperpolarizability; a reduction of 49% for anisotropy and an increase of 2% for the average linear polarizability. In solvent medium DMSO, we observed the change of Me to OMe, causing an increase of 2.13% for $\alpha(-\omega;\omega)$; a reduction of 61% for $\beta_{\|}z(-2\omega;\omega,\omega)$ an increase of 116% for $\beta_{\|}z(-\omega;\omega,0)$ a reduction of 3.8% for $\gamma(-2\omega;\omega,\omega,0)$ and a reduction of 2.8% for $\gamma(-\omega;\omega,0,0)$. The impact of replacing Me (compound I) with OMe (compound II) on the first hyperpolarizability is more important than the impact on the linear polarizability, which in turn is more important than on the dipole moment. All these properties saturated as the polarity increased, and we observed that the greater the polarity of the solvent, the higher these properties became. In addition, we also calculated the HOMO-LUMO Band-Gap energy of each compound, and we observed that the inclusion of the solvent medium in compound II caused a decrease in the Band-Gap energy, which corroborates the understanding that compound II has a higher first hyperpolarizability response. Furthermore, we observed that the effect of the transition between solvent media, polar to non-polar, did not significantly affect the Band-Gap energy values. These results are useful to understand the electronic effect of the change of substituent on the spectroscopic behavior of the compounds.

When we compare our results for the second hyperpolarizability (crystal) with those of a recent work on the crystal (*E*)-4-(3-fluorobenzyloxy)-*N*′-benzylidenebenzohydrazide [22], we see that our results are greater by 23.80% and 17.70% for compound I and compound II, respectively.

Finally, the results obtained for the two coumarin derivatives studied here show that these compounds constitute an attractive object for future studies of NLO properties, especially compound I because it presents higher values for the electric parameters. We hope that our results can provide significant information for further studies of these compounds for application as NLO materials.

Supplementary Materials: The following are available online at www.mdpi.com/2073-4352/7/6/158/s1: Table S1: MP2/6-311+G(d) results for the HOMO-LUMO for the compounds I; Table S2: MP2/6-311+G(d) results for the HOMO-LUMO for the compounds II; Table S3: The HOMO-LUMO frontiers orbitals for the coumarins compounds I and II in three different solvent media.

Acknowledgments: The authors would like to thank the following Brazilian agencies for financial support: Conselho Nacional de Desenvolvimento Científico e Tecnológico (CNPq), Coordenação de Aperfeiçoamento Pessoal de Nível Superior (CAPES) and Fundação de Apoio à Pesquisa do Estado de Goiás (FAPEG).

Author Contributions: Basílio Baseia, Francisco A. P. Osório and Clodoaldo Valverde conceptualization and methodology; Basílio Baseia, Francisco A. P. Osório, Larissa Ferreira Lima, and Clodoaldo Valverde analyzed the data; Basílio Baseia, Francisco A. P. Osório and Clodoaldo Valverde wrote the paper.

Conflicts of Interest: The authors declare no conflict of interest.

References

1. Al-Majedy, Y.K.; Kadhum, A.A.H.; Al-Amiery, A.A.; Mohamad, A.B. Coumarins: The Antimicrobial agents. *Syst. Rev. Pharm.* **2017**, *8*, 62–70. [CrossRef]
2. Anufrik, S.S.; Tarkovsky, V.V. 3-(2-Benzimidazolyl)coumarin derivatives—Highly effective laser media. *J. Appl. Spectrosc.* **2010**, *77*, 640–647. [CrossRef]
3. Yang, Y.; Zou, J.; Rong, H.; Qian, G.D.; Wang, Z.Y.; Wang, M.Q. Influence of various coumarin dyes on the laser performance of laser dyes co-doped into ORMOSILs. *Appl. Phys. B* **2007**, *86*, 309–313. [CrossRef]
4. Krystkowiak, E.; Dobek, K.; Maciejewski, A. Deactivation of 6-Aminocoumarin Intramolecular Charge Transfer Excited State through Hydrogen Bonding. *Int. J. Mol. Sci.* **2014**, *15*, 16628–16648. [CrossRef] [PubMed]
5. Wu, W.; Wang, J.; Zheng, Z.; Hu, Y.; Jin, J.; Zhang, Q.; Hua, J. A strategy to design novel structure photochromic sensitizers for dye-sensitized solar cells. *Sci. Rep.* **2015**, *5*, 8592. [CrossRef] [PubMed]
6. Zhang, X.; Zhang, J.-J.; Xia, Y.-Y. Molecular design of coumarin dyes with high efficiency in dye-sensitized solar cells. *J. Photochem. Photobiol. A Chem.* **2008**, *194*, 167–172. [CrossRef]
7. Hagberg, D.P.; Marinado, T.; Karlsson, K.M.; Nonomura, K.; Qin, P.; Boschloo, G.; Brinck, T.; Hagfeldt, A.; Sun, L. Tuning the HOMO and LUMO Energy Levels of Organic Chromophores for Dye Sensitized Solar Cells. *J. Org. Chem.* **2007**, *72*, 9550–9556. [CrossRef] [PubMed]
8. Kitamura, M.; Iwamoto, S.; Arakawa, Y. Enhanced light emission from an organic photonic crystal with a nanocavity. *Appl. Phys. Lett.* **2005**, *87*, 151119. [CrossRef]
9. Tanabe, T.; Notomi, M.; Mitsugi, S.; Shinya, A.; Kuramochi, E. All-optical switches on a silicon chip realized using photonic crystal nanocavities. *Appl. Phys. Lett.* **2005**, *87*, 151112. [CrossRef]
10. Soljacic, M.; Lidorikis, E.; Joannopoulos, J.D.; Hau, L.V. Ultralow-power all-optical switching. *Appl. Phys. Lett.* **2005**, *86*, 171101. [CrossRef]
11. Nozaki, K.; Tanabe, T.; Shinya, A.; Matsuo, S.; Sato, T.; Taniyama, H.; Notomi, M. Sub-femtojoule all-optical switching using a photonic-crystal nanocavity. *Nat. Photonics* **2010**, *4*, 477–483. [CrossRef]
12. Briseno, A.L.; Mannsfeld, S.C.B.; Reese, C.; Hancock, J.M.; Xiong, Y.; Jenekhe, S.A.; Bao, Z.; Xia, Y. Perylenediimide Nanowires and Their Use in Fabricating Field-Effect Transistors and Complementary Inverters. *Nano Lett.* **2007**, *7*, 2847–2853. [CrossRef] [PubMed]
13. Jazbinsek, M.; Mutter, L.; Gunter, P. Photonic Applications With the Organic Nonlinear Optical Crystal DAST. *IEEE J. Sel. Top. Quantum Electron.* **2008**, *14*, 1298–1311. [CrossRef]
14. Tan, L.; Jiang, W.; Jiang, L.; Jiang, S.; Wang, Z.; Yan, S.; Hu, W. Single crystalline microribbons of perylo[1,12-b,c,d]selenophene for high performance transistors. *Appl. Phys. Lett.* **2009**, *94*, 153306. [CrossRef]
15. Polisseni, C.; Major, K.D.; Boissier, S.; Grandi, S.; Clark, A.S.; Hinds, E.A. Stable, single-photon emitter in a thin organic crystal for application to quantum-photonic devices. *Opt. Express* **2016**, *24*, 5615. [CrossRef]
16. Zhang, L.; Pavlica, E.; Zhong, X.; Liscio, F.; Li, S.; Bratina, G.; Orgiu, E.; Samorì, P. Fast-Response Photonic Device Based on Organic-Crystal Heterojunctions Assembled into a Vertical-Yet-Open Asymmetric Architecture. *Adv. Mater.* **2017**, *29*, 1605760. [CrossRef] [PubMed]
17. Gomes, L.R.; Low, J.N.; Fonseca, A.; Matos, M.J.; Borges, F. Crystal structures of three 6-substituted coumarin-3-carboxamide derivatives. *Acta Crystallogr. Sect. E Crystallogr. Commun.* **2016**, *72*, 926–932. [CrossRef] [PubMed]
18. Frisch, M.J.; Trucks, G.W.; Schlegel, H.B.; Scuseria, G.E.; Robb, M.A.; Cheeseman, J.R.; Scalmani, G.; Barone, V.; Mennucci, B.; Petersson, G.A.; et al. *Fox, Gaussian 09, Revision A.1, (2009)*; Gaussian Inc.: Wallingford, CT, USA, 2009; Volume 139.
19. Santos, O.L.; Sabino, J.R.; Georg, H.C.; Fonseca, T.L.; Castro, M.A. Electric properties of the 3-methyl-4-nitropyridine-1-oxyde (POM) molecules in solid phase: A theoretical study including environment polarization effect. *Chem. Phys. Lett.* **2017**, *669*, 176–180. [CrossRef]
20. Santos, O.L.; Fonseca, T.L.; Sabino, J.R.; Georg, H.C.; Castro, M.A. Polarization effects on the electric properties of urea and thiourea molecules in solid phase. *J. Chem. Phys.* **2015**, *143*, 234503. [CrossRef] [PubMed]
21. Fonseca, T.L.; Sabino, J.R.; Castro, M.A.; Georg, H.C. A theoretical investigation of electric properties of L-arginine phosphate monohydrate including environment polarization effects. *J. Chem. Phys.* **2010**, *133*, 1–8. [CrossRef] [PubMed]

22. Rodrigues, R.F.N.; Almeida, L.R.; dos Santos, F.G.; Carvalho, P.S., Jr.; de Souza, W.C.; Moreira, K.S.; de Aquino, G.L.B.; Valverde, C.; Napolitano, H.B.; Baseia, B. Solid state characterization and theoretical study of non-linear optical properties of a Fluoro-*N*-Acylhydrazide derivative. *PLoS ONE* **2017**, *12*, e0175859. [CrossRef] [PubMed]
23. Valverde, C.; Rodrigues, R.F.N.; Machado, D.F.S.; Baseia, B.; de Oliveira, H.C.B. Effect of the crystalline environment on the third-order nonlinear optical properties of L-arginine phosphate monohydrate: A theoretical study. *J. Mol. Model.* **2017**, *23*, 122. [CrossRef] [PubMed]
24. Almeida, L.R.; Anjos, M.M.; Ribeiro, G.C.; Valverde, C.; Machado, D.F.S.; Oliveira, G.R.; Napolitano, H.B.; de Oliveira, H.C.B. Synthesis, structural characterization and computational study of a novel amino chalcone: A potential nonlinear optical material. *New J. Chem.* **2017**, *41*, 1744–1754. [CrossRef]
25. Vaz, W.F.; Custodio, J.M.F.; Silveira, R.G.; Castro, A.N.; Campos, C.E.M.; Anjos, M.M.; Oliveira, G.R.; Valverde, C.; Baseia, B.; Napolitano, H.B. Synthesis, characterization, and third-order nonlinear optical properties of a new neolignane analogue. *RSC Adv.* **2016**, *6*, 79215–79227. [CrossRef]
26. Ribeiro, G.C.; Almeida, L.R.; Napolitano, H.B.; Valverde, C.; Baseia, B. Polarization effects on the third-order nonlinear optical properties of two polymorphs of enamine derivative. *Theor. Chem. Acc.* **2016**, *135*, 244. [CrossRef]
27. Castro, A.N.; Almeida, L.R.; Anjos, M.M.; Oliveira, G.R.; Napolitano, H.B.; Valverde, C.; Baseia, B. Theoretical study on the third-order nonlinear optical properties and structural characterization of 3-Acetyl-6-Bromocoumarin. *Chem. Phys. Lett.* **2016**, *653*, 122–130. [CrossRef]
28. Guillaume, M.; Champagne, B.; Bégué, D.; Pouchan, C. Electrostatic interaction schemes for evaluating the polarizability of silicon clusters. *J. Chem. Phys.* **2009**, *130*, 134715. [CrossRef] [PubMed]
29. Kanoun, M.B.; Botek, E.; Champagne, B. Electrostatic modeling of the linear optical susceptibilities of 2-methyl-4-nitroaniline, m-nitroaniline, 3-methyl-4-nitropyridine *N*-oxide and 2-carboxylic acid-4-nitropyridine-1-oxide crystals. *Chem. Phys. Lett.* **2010**, *487*, 256–262. [CrossRef]
30. Seidler, T.; Champagne, B. Which charge definition for describing the crystal polarizing field and the χ (1) and χ (2) of organic crystals? *Phys. Chem. Chem. Phys.* **2015**, *17*, 19546–19556. [CrossRef] [PubMed]
31. Seidler, T.; Krawczuk, A.; Champagne, B.; Stadnicka, K. QTAIM-Based Scheme for Describing the Linear and Nonlinear Optical Susceptibilities of Molecular Crystals Composed of Molecules with Complex Shapes. *J. Phys. Chem. C* **2016**, *120*, 4481–4494. [CrossRef]
32. Seidler, T.; Stadnicka, K.; Champagne, B. Second-order Nonlinear Optical Susceptibilities and Refractive Indices of Organic Crystals from a Multiscale Numerical Simulation Approach. *Adv. Opt. Mater.* **2014**, *2*, 1000–1006. [CrossRef]
33. Seidler, T.; Stadnicka, K.; Champagne, B. Evaluation of the Linear and Second-Order NLO Properties of Molecular Crystals within the Local Field Theory: Electron Correlation Effects, Choice of XC Functional, ZPVA Contributions, and Impact of the Geometry in the Case of 2-Methyl-4-nitroaniline. *J. Chem. Theory Comput.* **2014**, *10*, 2114–2124. [CrossRef] [PubMed]
34. Seidler, T.; Stadnicka, K.; Champagne, B. Linear and second-order nonlinear optical properties of ionic organic crystals. *J. Chem. Phys.* **2014**, *141*, 104109. [CrossRef] [PubMed]
35. Seidler, T.; Stadnicka, K.; Champagne, B. Investigation of the linear and second-order nonlinear optical properties of molecular crystals within the local field theory. *J. Chem. Phys.* **2013**, *139*, 114105. [CrossRef] [PubMed]
36. Kleinman, D.A. Nonlinear Dielectric Polarization in Optical Media. *Phys. Rev.* **1962**, *126*, 1977–1979. [CrossRef]
37. Nkungli, N.K.; Ghogomu, J.N. Concomitant Effects of Transition Metal Chelation and Solvent Polarity on the First Molecular Hyperpolarizability of 4-Methoxyacetophenone Thiosemicarbazone: A DFT Study. *J. Theor. Chem.* **2016**, *2016*, 1–19. [CrossRef]
38. Pluta, T.; Sadlej, A.J. Electric properties of urea and thiourea. *J. Chem. Phys.* **2001**, *114*, 136. [CrossRef]
39. Song, X.; Farwell, S.O. Pyrolysis gas chromatography atomic emission detection method for determination of N-containing components of humic and fulvic acids. *J. Anal. Appl. Pyrolysis* **2004**, *71*, 901–915. [CrossRef]
40. Raj, R.K.; Gunasekaran, S.; Gnanasambandan, T.; Seshadri, S. Combined spectroscopic and DFT studies on 6-bromo-4-chloro-3-formyl coumarin, Spectrochim. *Acta Part A Mol. Biomol. Spectrosc.* **2015**, *139*, 505–514. [CrossRef] [PubMed]